International Journal of Mass Spectrometry 295 (2010) 85–93

Contents lists available at ScienceDirect

International Journal of Mass Spectrometry

journal homepage: www.elsevier.com/locate/ijms

Fragmentation pathways of eight nitrogen-containing bisphosphonates (BPs) investigated by ESI-MS^n in negative ion mode

Zhibo Qu[a], Xiaolan Chen[a,*], Chen Qu[b], Lingbo Qu[a,c], Jinwei Yuan[c], Donghui Wei[a], Huina Li[a], Xiaoying Huang[a], Yuqin Jiang[a], Yufen Zhao[a,d,*]

[a] Department of Chemistry, Zhengzhou University, Key Laboratory of Chemistry Biology and Organic Chemistry, Daxue Road No. 75, Zhengzhou, Henan 450052, China
[b] College of Chemistry, Nankai University, Tianjin 300071, China
[c] School of Chemistry & Chemical Engineering, Henan University of Technology, Zhengzhou 450001, China
[d] Department of Chemistry, Xiamen University, Xiamen 361005, China

ARTICLE INFO

Article history:
Received 3 May 2010
Received in revised form 10 July 2010
Accepted 12 July 2010
Available online 16 July 2010

Keywords:
Nitrogen-containing bisphosphonate
ESI-MS^n
Fragmentation pathway
Diagnostic ion
Theoretical calculation

ABSTRACT

Fragmentation pathways of eight nitrogen-containing bisphosphonates (BPs), including Pamidronate, Alendronate, and five corresponding acylated derivatives, and Risedronate, were investigated by electrospray ionization mass spectrometry (ESI-MS) in conjunction with tandem mass spectrometry in negative ion mode. Characteristic fragment ions involved were formed by successive loss of water molecules, including α, β-unsaturated product ions formed by dehydration of the α-hydroxyl group and β-hydrogen, cyclic ions with P–O–P four-membered rings formed by dehydration of the two –OH groups attached to two phosphorus atoms, and cyclic phosphoramide ions with five- or six-membered rings formed by loss of water via an intramolecular nucleophilic substitution reaction, in which $–NH_2$ (or –NH–) group on γ or δ carbon acted as the nucleophile to attack phosphorus atom of P═O group at the initial stage. Another notable characteristic product ion $[HP_2O_5]^-$ at *m/z* 143, shown by all eight ESI-MS^2 spectra, is a diagnostic ion of bisphosphonate group, formed from the four-membered ring ion containing P–O–P. Some additional fragmentation ions were produced from chloroacetyl Alendronate, chloroacetyl Pamidronate, and Risedronate containing triple bond ions, formed by loss of water from the corresponding enol anions. The hydrogen/deuterium (H/D) exchange experiment, theoretical calculations, and the high-resolution mass spectrometry were appropriately employed to rationalize the proposed fragmentation pathways.

1. Introduction

Bisphosphonates (BPs) or diphosphonates, are a class of drugs that prevent the loss of bone mass, used to treat osteoporosis and similar diseases. More recently, BPs have been used to reduce fracture rates in children with osteogenesis imperfecta [1] and in treatment of otosclerosis [2]. BP inhibits osteoclastic bone resorption both in vivo and in vitro [3,4]. The typical structure of BP is generally similar to that of pyrophosphate. The only difference is that the oxygen atom that binds the two phosphorus atoms in pyrophosphate (P–O–P) is replaced by a carbon (P–C–P). The carbon between the two phosphorous atoms is generally attached to two additional side-chains in their molecules which are not present in pyrophosphate. In general, there is a hydroxyl attached to the central (geminal) carbon atom [5], which enhances the affinity of BPs for calcium crystals, and a nitrogen atom-containing carbon chain enhances their potency and determines their mechanism of action. The structural features of BPs have led to the synthesis of a large number of compounds with different properties [6–8]. The greatest improvements in the biological activities of BPs have resulted from the introduction of a basic nitrogen atom into the side chain on the geminal carbon. Further jumps in the activity in bone resorption were obtained by transposing the amine group farther from the "bone hook" or by alkylating the primary amine to a tertiary one [9]. The nitrogen-containing BPs are the latest and most potent addition to this family of BPs. They have high potency, and are specially targeted to the osteoclast on bone with very low doses (5–10 mg clinically) [10]. Nitrogen-containing BPs act on bone metabolism by binding and blocking the enzyme farnesyl diphosphate synthase (FPPS) in the HMG-CoA reductase pathway (also known as the mevalonate pathway) [11].

Electrospray ionization multistage tandem mass spectrometry (ESI-MS^n), a powerful tool for structure determination, has been widely used in chemistry, biochemistry and pharmaceutical research [12–14]. However, only a few methods based upon mass spectrometric detection have been reported for BPs. For example,

* Corresponding authors at: Key Laboratory of Chemical Biology and Organic Chemistry of Henan Province, Department of Chemistry, Zhengzhou University, Zhengzhou 450052, China. Tel.: +86 371 67767051; fax: +86 371 67767051.
E-mail address: chenxl@zzu.edu.cn (X. Chen).

1387-3806/$ – see front matter
doi:10.1016/j.ijms.2010.07.017

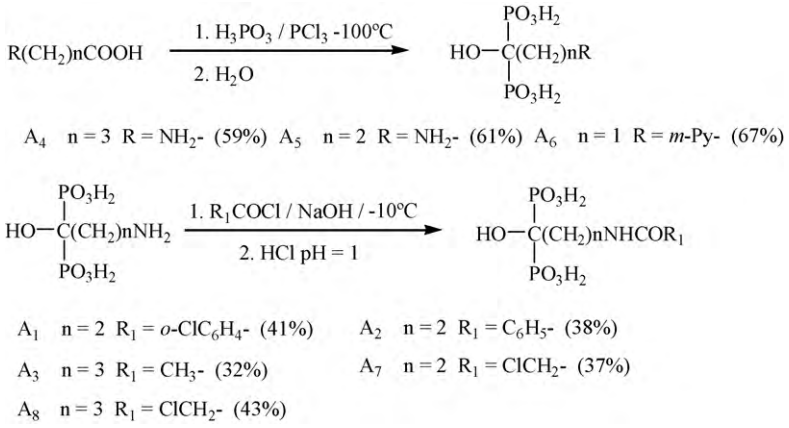

Scheme 1. Synthesis of nitrogen-containing BPs (A_1–A_8).

only the mass spectrometric (MS) behavior and fragmentation of a relatively simple bisphosphonate of clodronate, in which there are two chloro groups attached to the geminal carbon atom, were reported by Risto Kostiainen's group [15]. Electrospray ionization mass spectrometric (ESI-MS^n) fragmentation of the very important nitrogen-containing BPs has not been reported in previous literature. In the study described in this paper, eight nitrogen-containing BPs were synthesized by reference to the literature [16] and the fragmentation patterns were investigated by electrospray ionization multistage tandem mass spectrometry (ESI-MS^n) in negative ion mode in details. The hydrogen/deuterium (H/D) exchange experiment, theoretical calculations, and the high-resolution mass spectrometry were appropriately employed to rationalize the proposed fragmentation pathways.

2. Experimental

2.1. Chemicals and synthesis of bisphosphonates

Amino acids were purchased from Sino-American Biotechnology Co. (Shanghai, China). Deuterated solvents D_2O were from Beijing Chemical Factory (Beijing, China). Other reagents were purchased from Sinopharm Chemical Reagent Co., Ltd. (Shanghai, China).

Experimental BPs were prepared by the method described previously. Compounds containing a carboxylic functional group (0.025 mol), including two amino acids and pyridin-3-yl-acetic acid, were mixed with phosphorus acid (0.0375 mol) and then stirred for 1 h at 90 °C. Phosphorus trichloride (0.05 mol) was added dropwise to the suspension at 100 °C under stirring. After 4 h, the solution was cooled down to room temperature. The residue was hydrolyzed by adding 10 mL H_2O, the solution decolorized by an appropriate amount of activated carbon was added to 150 mL isopropanol, then white flocculent products were precipitated very quickly. The crude product was filtrated and washed three times with water. Compounds (A_4–A_6) were obtained. Place compound A_4 or A_5 (10 mmol), acyl chloride (20 mmol), and 12 mL (3.5%) NaOH in the flask and cool it to −10 °C in an ice-salt bath, then stir for 6 h. Using (1 mol/L) HCl to adjust to pH = 1, then pour it into 200 mL of ethanol. The white deposit appeared quickly and was distilled. The residue was then purified by recrystallization from CH_3OH:H_2O = 1:1 (v/v). The white crystals (A_1, A_2, A_3, A_7 and A_8) were obtained in moderate yields (shown in the brackets, Scheme 1). All of samples were synthesized as shown in Scheme 1. The structrues were confirmed by ^{31}P NMR, ^{1}H NMR, ^{13}C NMR and ESI-MS.

2.2. Mass spectrometric conditions

The ESI mass spectra of BPs were acquired on an Esquire 3000 ESI-MS with an ion trap mass spectrometer in negative ionization mode (Bruker Daltonik Gmbh, Germany). The MS^n spectra were obtained by collision-induced dissociation (CID) with helium after isolation of the appropriate precursor ions. Ionization of analysis was carried out using the following setting of the ESI: nebulizer gas flow 7 psi, dry gas 4.5 L/min, dry temperature 300 °C, spray voltage 4 kV. Samples were dissolved in CH_3OH:H_2O = 1:1 (v/v) and ionized by electrospray ionization. Calibration of m/z was performed using a standard ESI-tuning-mixture. Scan range was 50–500 m/z and scan resolution was normal (13,000 m/z/s).

High-resolution mass spectra were performed on a Micromass Q-TOF MicroTM mass spectrometer with an ESI source (Waters, Manchester, UK). Argon was used as the collision gas. Nitrogen was used as the nebulizer and dissolvation gas. The ESI source was operated in negative ion mode with optimized conditions. The mass spectra over the mass range 50–500 with a capillary voltage of 3.5 kV, a cone voltage of 25 V, a source temperature of 80 °C, a dissolvation temperature of 170 °C, a collision voltage of 7 V, a cone gas flow of 50 L/h and a dissolvation gas flow of 350 L/h. During the MS/MS experiments, the deprotonated A_1 was chosen as precursor ion and isolated in the quadruple.

2.3. Computational details

To simplify the calculations, compound A_1 was chosen as a model. Using density functional theory, the geometries of the reactant, intermediates and products in all reaction channels were optimized at the B3LYP/6-31G (d, p) level. All theoretical calculations were performed using the GAUSSIAN03 [17] suite of software.

3. Results and discussion

ESI-MS spectra in most cases, were acquired in positive ion mode to produce $[M+Na]^+$ and $[M+H]^+$ ions. However, four acidic hydroxyl groups of BPs can be easily deprotonated to obtain the conjugate anions in ionization process. Positive ionization by protonization was not observed in any case and higher sensitivity was obtained by negative ionization. ESI-MS^n spectra of compounds A_1–A_8 in negative mode were studied in detail and the data are shown in Table 1. The most representative fragmentation ways were shown in Scheme 2. The main fragment ions derived from $[M-H]^-$ ion were $[M-H-H_2O]^-$, $[M-H-2H_2O]^-$, $[M-H-H_3PO_3]^-$ and $[HP_2O_5]^-$ ions. There were three ways to lose the first molecule of water. The relatively stable α, β-unsaturated product ion ($\mathbf{a_1}$)

Table 1
Negative ion ESI-MS^n of $[M-H]^-$ ions of compounds A_1–A_8 [m/z (relative abundance, %), m = MW − 1].

Com.	Precursor ions	Fragment ions										
		a (m-18)	**b** (m-36)	**c** (m-82)	**d**	**e** (b-64)	**f** (d-64)	**g** (m-54)	**h**	**i**	**j**	
	372	354 (21)	336 (21)	290 (100)	143 (11)							
	354		336 (22)	290 (100)	143 (14)							
A1	336			290 (7)		272 (100)				127 (28)		
	290								135 (100)			
	143						79 (100)					
	338	320 (57)	302 (6)	256 (100)	143 (5)							
	320		302 (30)	256 (100)	143 (7)							
A2	302					238 (100)				127 (64)		168 (14)
	256								135 (100)			
	143						79 (100)					
	276	258 (49)	240 (33)	194 (100)	143 (22)	176 (14)						
	258		240 (61)	194 (100)	143 (31)	176 (48)	79 (9)					211 (14)
A3	240					176 (100)				127 (33)		137 (7)
	194								135 (100)		63 (28)	
	143						79 (100)					
	248	230 (69)	212 (100)	166(50)	143(19)	148 (42)	79 (12)	194 (72)				
	230		212 (95)			148 (19)		194 (100)				166 (10)
	212					148 (19)		194 (100)				
A4	194						79 (100)					
	166					148 (100)						
	148						79 (100)				63 (25)	
	143						79 (100)					
	234	216 (100)	198 (58)	152 (43)	143 (10)							
	216		198 (100)	152 (23)		134 (13)	79 (14)			127 (5)		
A5	198					134 (67)		180 (7)				
	152					134 (100)					63 (38)	
	143						79 (100)					
	282	264 (46)	246 (71)	200 (100)	143 (9)					127 (6)		
	264		246 (100)	200 (25)	143 (11)					127 (18)		
A6	246									127 (100)		
	200							182 (59)			63 (100)	
	143						79 (100)					
	310	292 (45)	274 (23)	228 (100)	143 (15)	210 (3)						192 (8)
	292		274 (57)	228 (100)	143 (5)	210 (13)			135 (3)			256(8) 192 (6)
	274					210 (100)				127 (16)		
A7	228								136 (29)			192 (100)
	210											192 (6) 174(25) 131 (8)
	192									136 (40)		
	143						79 (100)					
	324	306 (16)	288 (8)	242 (100)	143 (17)			270 (11)				252 (15) 206 (10)
	306		288 (33)	242 (100)	143 (52)			270 (38)		127 (10)		252 (24) 224 (10) 194 (14)
	288							270 (26)				252 (97) 224 (100)
												188 (60)
A8	270											252 (100)
	252											188 (100)
	242											206 (100) 81(14) 121 (29)
	206						79 (2)					121 (100)
	143						79 (100)					

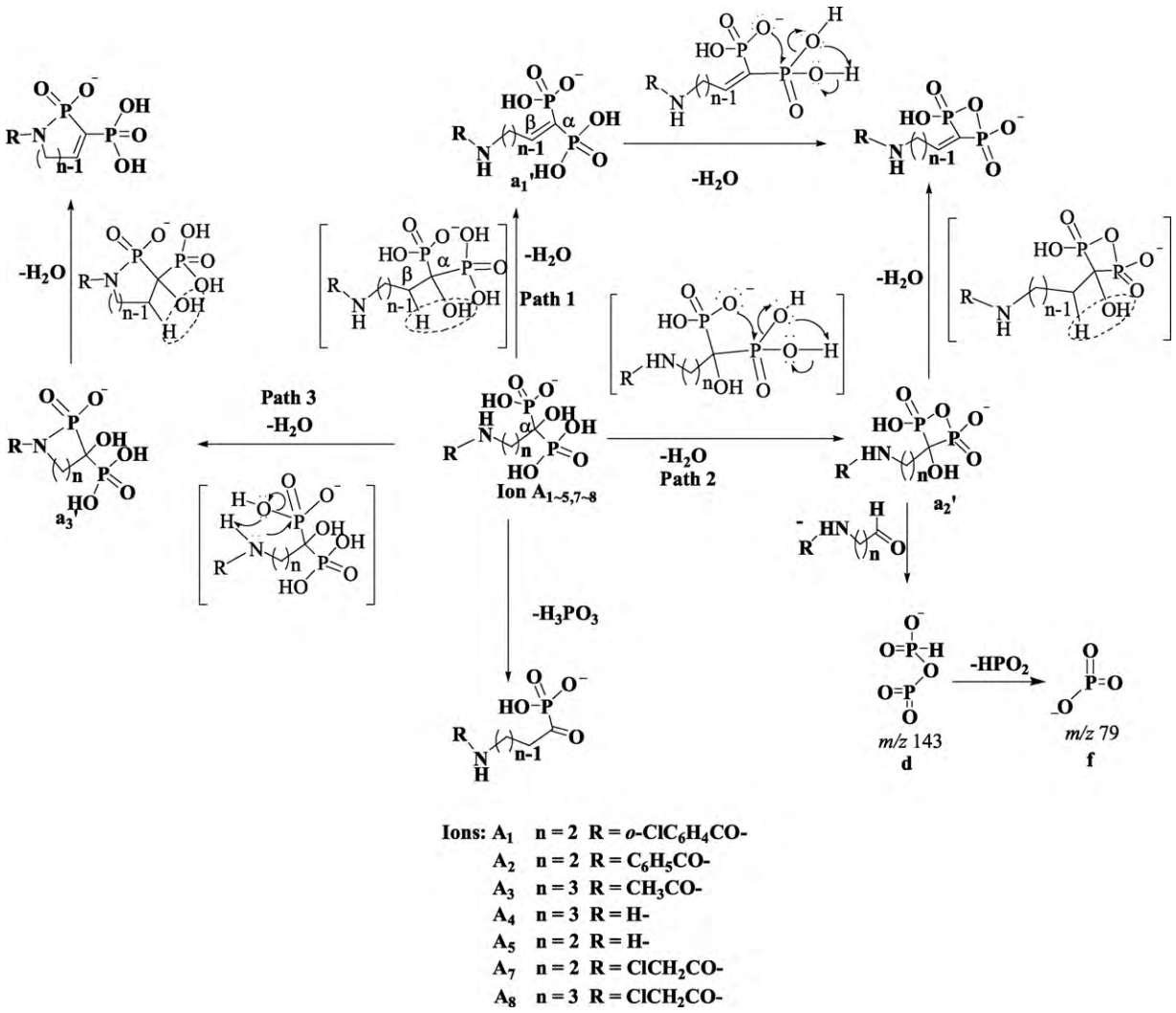

Scheme 2. Main fragment pathways of nitrogen-containing BPs.

was produced by dehydration of the –OH at α carbon atom and the –H group at β carbon atom (Path 1). The four-membered ring ion containing P–O–P (**a_2**) was produced by dehydration of the two –OH groups attached to two phosphorous atoms separated by a carbon atom (Path 2). The cyclic phosphoramide ion with a five- or six-membered ring (**a_3**) was produced by loss of water via a nucleophilic addition–elimination mechanism, in which $–NH_2$ (or –NH–) group on γ ($n = 2$) or δ ($n = 3$) carbon acted as the nucleophile to attack phosphorous atom of P═O group at the initial stage (Path 3). Supports for the three dehydrated ways resulted from further fragmentation pathway analyses about precursor ion $[M–H–2H_2O]^-$ as illustrated in Scheme 3 in the following. $[HP_2O_5]^-$ ion at *m/z* 143 (**d**) is the most characteristic product ion shown by all eight ESI-MS^2 spectra, formed spontaneously from the four-membered ring ion containing P–O–P (**a_2**) by loss of an aldehyde. Therefore, $[HP_2O_5]^-$ ion at *m/z* 143 can hopefully be treated as a diagnostic ion of bisphosphonate group. The further fragment ion at *m/z* 79 (**f**) can be formed from the ion at *m/z* 143 by losing HPO_2. A_7 and A_8 ions showed some additional fragmentation pathways, arising from extra fragmentation of acyl parts, including a triple bond ion derived from their enol ions by loss of a molecule of water (Scheme 4). The ESI mass spectral fragmentation pathways of compound A_1, A_6 and A_8 are discussed as typical examples in details. Besides the common fragmentation pathways mentioned above, the different fragmentation pathways induced by the difference among the structures of the BPs would also be presented and analyzed in the following using three typically related examples of compound A_1, A_6 and A_8, based on the fact that the similar fragmentation pathways were shown by Compounds A_1–A_5 and the similar fragmentation pathways by Compounds A_7 and A_8, as concluded in Table 1.

The ESI-MS^n fragmentation of deprotonated A_1 at *m/z* 372 (Fig. 1(**1**)) is summarized in Scheme 3. The ESI-MS^2 of the ion at *m/z* 372 produced the product ion at *m/z* 354, corresponding to $[M–H–H_2O]^-$, assigned as **a_1**, **a_2**, and **a_3** ions based on three different dehydrated ways. Ion at *m/z* 336 was corresponding to $[M–H–2H_2O]^-$, assigned as **b_1** and **b_2** ions in accordance with further dehydration of **a_1**, **a_2**, and **a_3** ions. The product ion **c** at *m/z* 290 was corresponding to $[M–H–H_3PO_3]^-$. The most characteristic product ion **d** concerning the biphosphonate part at *m/z* 143 was formed by losing an aldehyde $C_{10}H_{10}ClNO_2$ from the cyclic ion **a_2**. The existing of *m/z* 143 supports the Path 2 and the structure of product ions, based on the fragmentation pathways shown in Scheme 2 and 3. ESI-MS^3 spectrum (Fig. 1(**2**)) of the ion at *m/z* 354, corresponding to $[M–H–H_2O]^-$ was shown in Fig. 1(**2**). Three ions at *m/z* 336, *m/z* 290 and *m/z* 143 were produced from the ion at *m/z* 354. The product ions **c** at *m/z* 290 and **d** at *m/z* 143, were produced by Path 2 from fragmentation of the ion **a_2** at *m/z* 354 by losing HPO_2 and an aldehyde $C_{10}H_{10}ClNO_2$, respectively. The product ion **b_1** at *m/z* 336 can be formed by losing water from the ion **a_1** at *m/z*

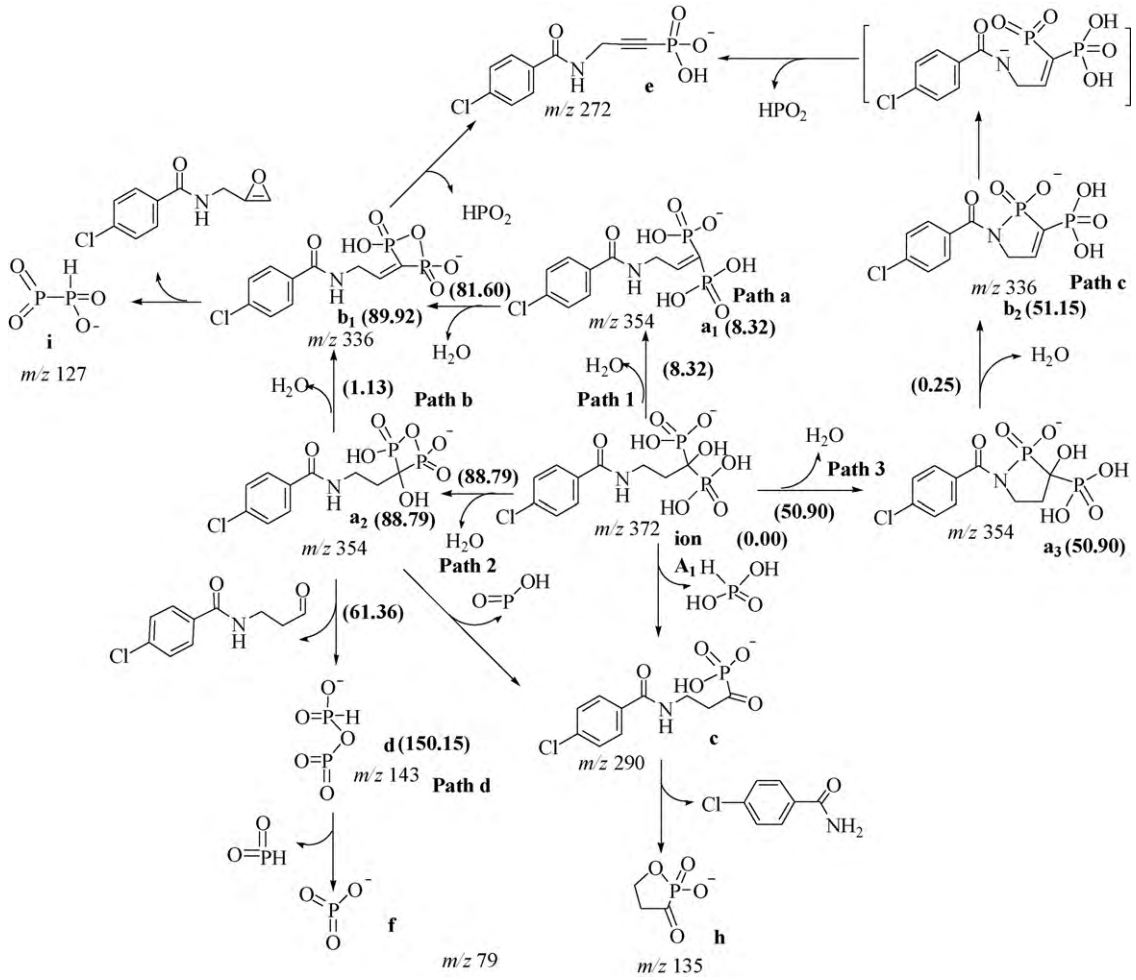

Scheme 3. Proposed fragment pathways of deprotonated A_1. The values next to the arrows (in kJ/mol) represent the relative Gibbs free energies (ΔG) for each individual fragmentation reaction.

354 by Path 1 or from the ion $\mathbf{a_2}$ at m/z 354 by Path 2, meanwhile ion $\mathbf{b_2}$ at m/z 336 can be formed by successive losing water from the ion $\mathbf{a_3}$ at m/z 354 as shown in Scheme 3. ESI-MS^3 spectrum of the ion at m/z 336 was shown in Fig. 1(**3**). Two ions at m/z 272, m/z 127 were produced from the precursor ion at m/z 336. It is especially worth mentioning that ion **e** can be reasonably formed by loss of HPO_2 not only from ion $\mathbf{b_1}$ produced by Path 1 and 2, but also from the ion $\mathbf{b_2}$ produced by Path 3, giving an important support for the Path 1 and 3. Moreover the easy formation of cyclic phosphoramide ion with a five- or six-membered ring, corresponding to the first water loss ion $\mathbf{a_3}$, admittedly results from the extraordinary stability of a five- or six-membered ring structure. The existing of m/z 143 mentioned in our manuscript supports the Path 2 and especially supports the structure of product ion $\mathbf{a_2}$ with four-membered ring. To a great extent, the γ- or δ-cyclic phosphoramide ion $\mathbf{a_3}$ with a five- or six-membered ring should be favorably formed under the mass spectral condition, based on the premise that product ion $\mathbf{a_2}$ with four-membered ring can be formed in this circumstance. The ion **i** at m/z 127, corresponding to the low-intensity of peak of ESI-MS^3 spectrum, was reasonably produced from the ion $\mathbf{b_1}$ by loss of a molecule $C_{10}H_8ClNO_2$, giving an assistant support for Path 1. The ESI-MS^3 spectrum of the ion at m/z 290 was shown in Fig. 1(**4**). The ion with P–O bond five-member ring at m/z 135 was assigned as **h** produced by loss of a molecular of *p*-chlorobenzamide. The ESI-MS^3 spectrum of the ion at m/z 143 was shown in Fig. 1(**5**). The ion at m/z 79 was assigned as **f** formed by losing HPO_2 from the parent ion at m/z 143. It is also worth mentioning that the ions **i**, **h** and **e**, from the corresponding ESI-MS^3 spectra, respectively, were additional ions besides the common fragmentation ions shown in Scheme 2.

The analysis showed that the main fragment pathways of compound A_8 were in good agreement with the characteristic fragment pathways of nitrogen-containing BPs. Besides similar fragmentation patterns shown by compound A_{1-5}, Compounds A_7 and A_8 displayed additional fragmentation pathways owing to the acyl group of the two molecules. Herein compound A_8 was discussed as an example (Scheme 4). Ions at m/z 306 and at m/z 288 were corresponding to $[M-H-H_2O]^-$ and $[M-H-2H_2O]^-$, respectively. The product ion at m/z 242 was corresponding to $[M-H-H_3PO_3]^-$. The diagnostic ion at m/z 143 was also observed. The product ion at m/z 79 was formed by losing HPO_2 from the parent ion at m/z 143. In addition, the ion peaks at m/z 270 and m/z 252, corresponding to $[M-H-3H_2O]^-$, assigned as **g** (keto ion) and **k** (enol ion), and $[M-H-4H_2O]^-$, assigned as **l**, were observed. The ion **n** at m/z 188 was reasonably produced from the ion **l**, the ion **l** from the enol ion **k** at m/z 270, the keto ion **g** at m/z 270 from the ion $\mathbf{b_2}$ at m/z 288, and the ion $\mathbf{b_2}$ at m/z 288 from the ion $\mathbf{a_3}$ at m/z 306 following Path 3. Again, the existing of ions **n**, **l**, **k**, **g** strongly support the Path 3 and the structure of the product ions. Some other additional ions were formed as shown in Table. 1 and Scheme 4, including the ion at m/z 81 formed by loss of $C_7H_9ClO_2$ from the ion at m/z 242, the ion at m/z 206 formed from the ion at m/z 242 by losing a molecule of HCl and the ion at m/z 121 formed by losing a molecule of C_4H_7NO from the ion at m/z 206. The existence of the enol ion (**k**) was supported

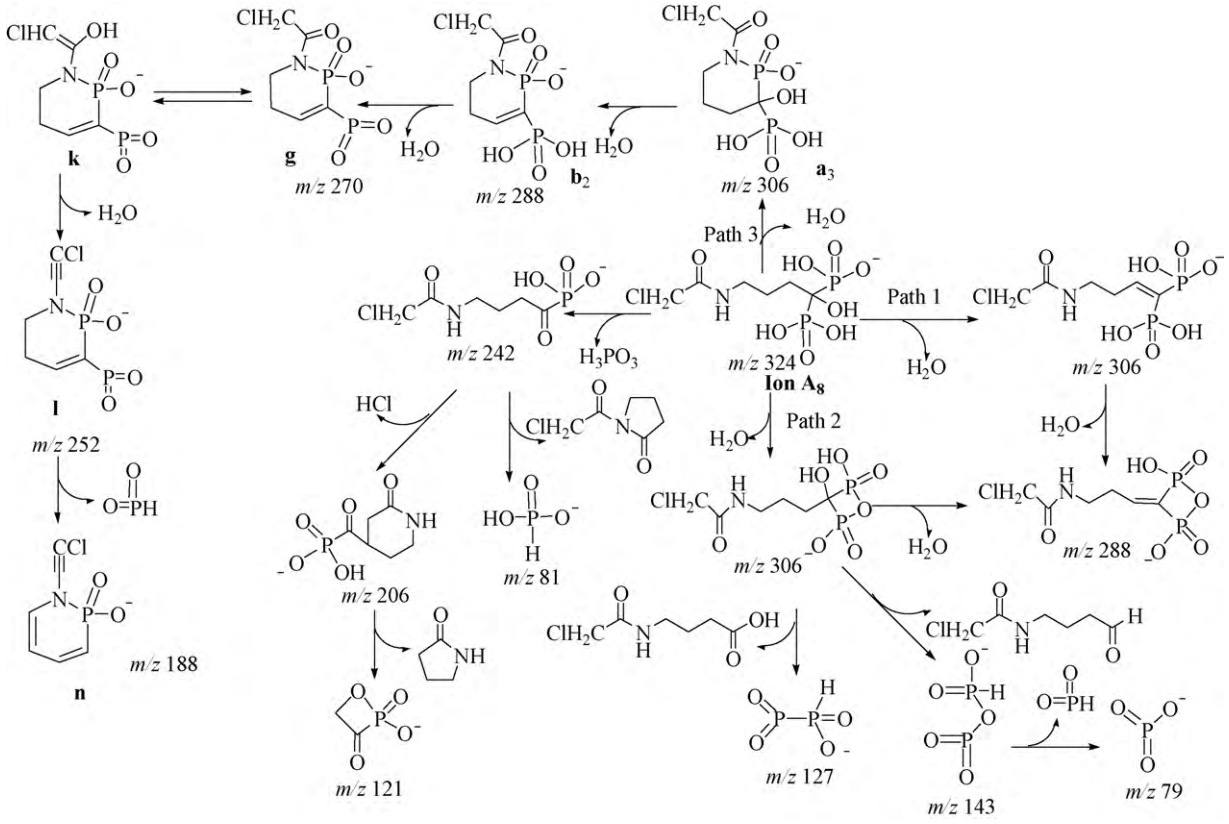

Scheme 4. Proposed fragmentation pathways of compound A_8.

by further hydrogen/deuterium (H/D) exchange experiment as the following.

Compound A_8 was dissolved in the D_2O and shaken for 1 h to ensure the active hydrogens were exchanged as much as possible. Then the solution was analyzed by ESI tandem mass spectrometry in negative mode. The corresponding ESI-MS^4 spectrum of the ion around 270 of compound A_8 was shown in Fig. 2. The peak at *m*/*z* 271 should be corresponded to the deuterated enol or keto ion, and the peak at *m*/*z* 270 should be corresponded to the non-deuterated keto or enol ion. The deuterated enol or keto ion must be formed through an equilibrium established between the enol and keto forms. The deuterium experiment could give a support for the existence of its enol form. The existence of its enol form at *m*/*z* 270 can favorably result in the formation of the ion at *m*/*z* 252 by dehydration.

The relatively higher activity attained to data has been with the nitrogen-containing heterocyclic BP, Risedronate [18]. The ESI-MS^n spectra of Risedronate (A_6) showed fewer fragmentation peaks in comparison with the other seven BPs containing long chain. Most representative fragmentation patterns of seven BPs mentioned above were also found in that of Risedronate, as shown in Scheme 5. Ions at *m*/*z* 264 and at *m*/*z* 246 were corresponding to $[M-H-H_2O]^-$ and $[M-H-2H_2O]^-$, respectively. The product ion at *m*/*z* 290 was corresponding to $[M-H-H_3PO_3]^-$. The most characteristic product ion at *m*/*z* 143 was also observed from the cyclic ion at *m*/*z* 246. Additionally, a specific ion at *m*/*z* 182 was produced by elimination of water from the enolate anion at *m*/*z* 200.

In order to investigate the reason for the above different fragmentation pathways of losing water molecules, the structures and energies of those deprotonated ions were optimized and calculated by density functional theory at the B3LYP/6-31G (d, p) level using Gaussian 03 software. It is considered that in CID-ESI-MS process, the energy that is transferred to the precursor ion owing to the collision activation can even surpass the activation barrier for some specific fragmentation reactions. The difference between the initial and final energy states can be used to understand the mechanism, and it is not necessary to consider the energies of any transitions state species [19]. Therefore, the relative Gibbs free energies of compound A_1, which represent four different pathways **a**, **b**, **c**, and **d**, respectively, were calculated. The deprotonated compound A_1 was assumed as 0.00 kJ/mol and the data of calculation have been shown in Scheme 3. The formation of the ion $\mathbf{a_3}$ from the deprotonated molecule **A** is an endergonic process, as evidenced by the relative energies of **A** (0.00 kJ/mol) and $\mathbf{a_3}$ (50.90 kJ/mol). Moreover, the ion $\mathbf{a_3}$ can easily transform to $\mathbf{b_2}$ (0.25 kJ/mol) via path c. Furthermore, the ion $\mathbf{a_1}$ (8.32 kJ/mol) is the most easily transformed from the ion **A** by losing one water molecule, so the path a is a more thermodynamically favored process, thus, the ion **A** does not easily transform to the ion $\mathbf{a_2}$ (88.79 kJ/mol). The ion $\mathbf{b_1}$ (1.13 kJ/mol) can easily be formed from the ion $\mathbf{a_2}$ via path b, however, the formation of the ion **d** from the precursor ion $\mathbf{a_2}$ need 61.36 kJ/mol via path d, that is why the relative abundances of the ion **d** is relatively lower than other ions. As concerned as above, all the theoretical calculations are in good agreement with the experimental results. Noteworthy, the results of theoretical calculations successfully demonstrated that their fragment ions can be rationalized on the basis of the relative Gibbs free energies.

To certify the proposed structure of the ions produced from the parent ion $[M_{A1}-H]^-$, the mass-to-charge ratios of the fragment ions were measured using the ESI-Q-TOF (Table 2). The correlation between the theoretical and measured values supports the proposal fragmentation of compound A_1.

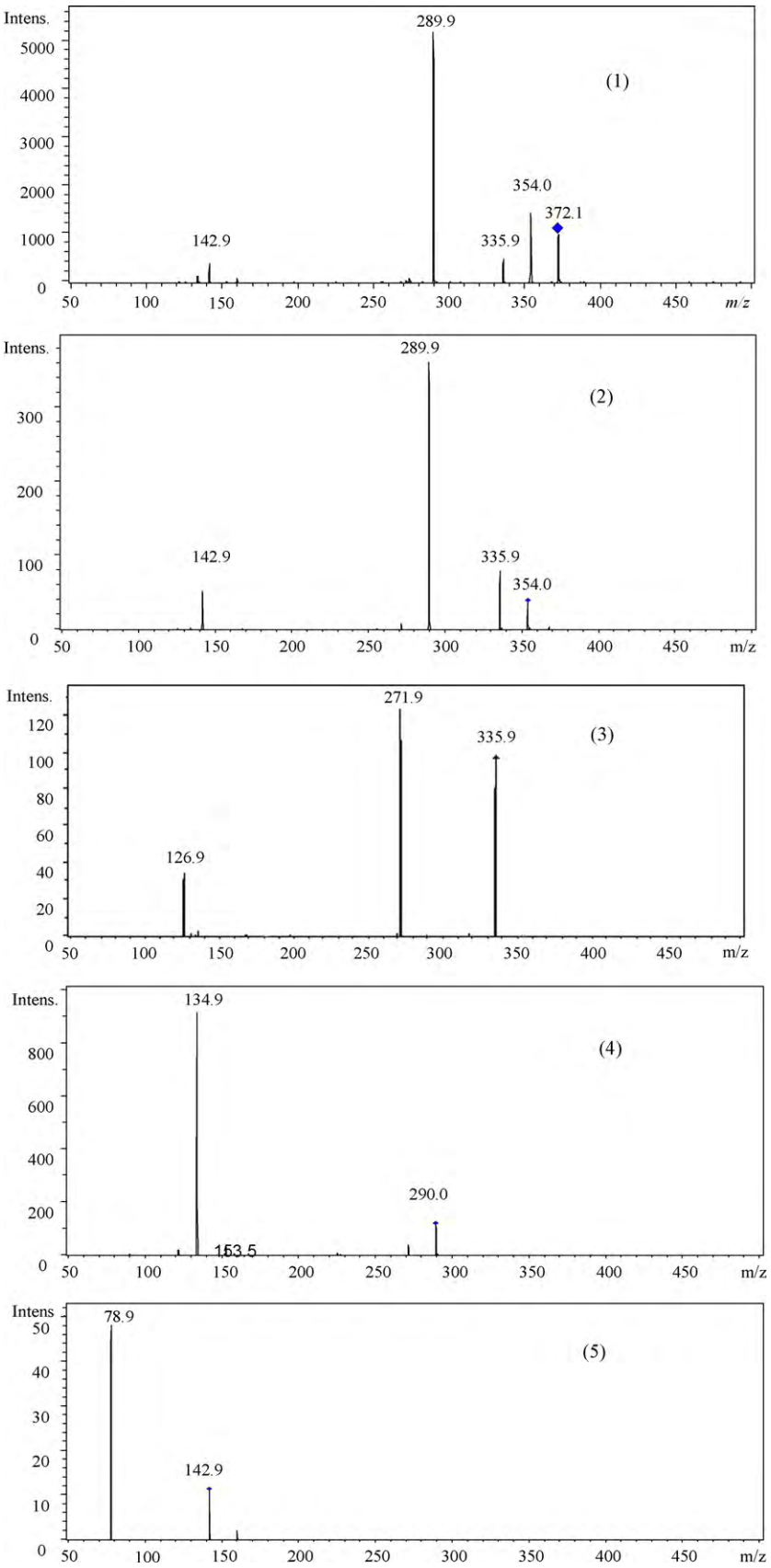

Fig. 1. (**1**) ESI-MS^2 of $[M-H]^-$ at m/z 372 of compound A_1. (**2**) ESI-MS^3 of the ion at m/z 354. (**3**) ESI-MS^3 of the ion at m/z 336. (**4**) ESI-MS^3 of the ion at m/z 290. (**5**) ESI-MS^3 of the ion at m/z 143.

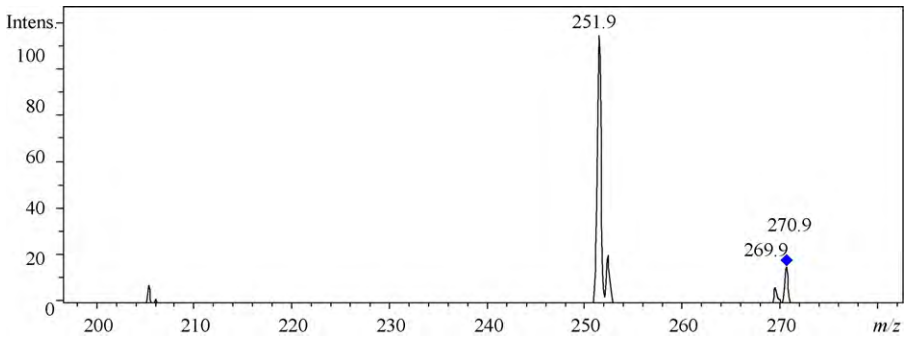

Fig. 2. Expanded ESI-MS^4 spectrum of the ion at m/z 270 of deuterated compound A_8.

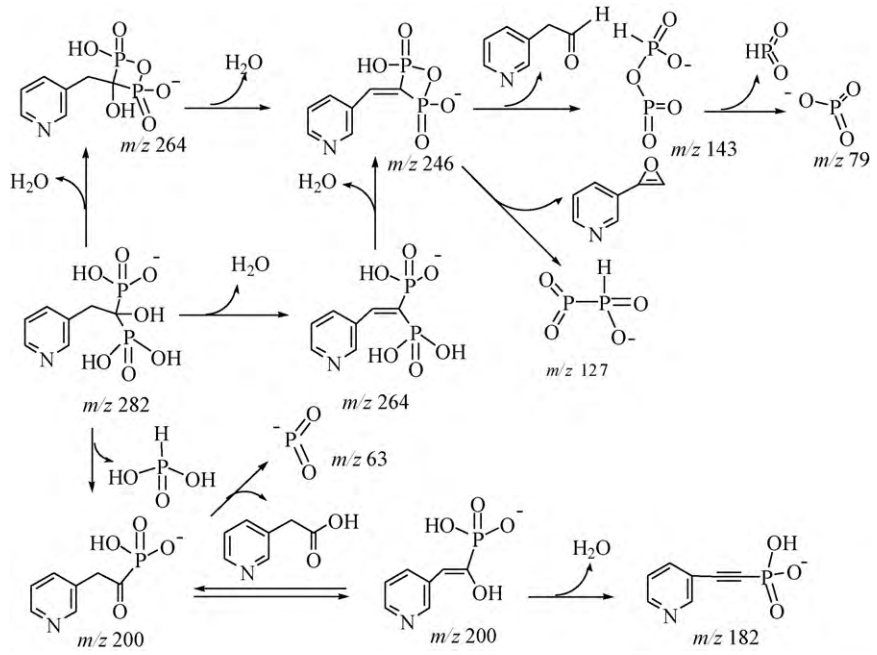

Scheme 5. Proposed fragmentation pathways of compound A_6.

Table 2
High-resolution mass spectral data for the main ions of A_1 (Obtained with ESI-MS^2 in the negative ion mode).

Ion species	Theoretical mass (m/z)	Measured mass (m/z)	Relative error (ppm)
$[M-H]^-$	371.9810	371.9801	2.4
$[M-H-H_2O]^-$	353.9705	353.9693	2.2
$[M-H-H_2O-H_2O]^-$	335.9599	335.9607	2.3
$[M-H-H_3PO_3]^-$	289.9991	290.0004	4.4
$[M-H-H_2O-C_{10}H_{10}ClNO_2]^-$	142.9305	142.9312	4.8

4. Conclusions

In conclusion, the negative ion electrospray ionization mass spectral fragmentation pathways of BPs, including seven nitrogen-containing side chain BPs and one nitrogen-containing heterocyclic BP, were analyzed by multistage mass spectrometry. The abundant fragment ions were observed by successive loss one or two molecules of water. The most representative fragmentation ions derived from $[M-H]^-$ ion were $[M-H-H_2O]^-$, $[M-H-2H_2O]^-$, $[M-H-H_3PO_3]^-$ and $[HP_2O_5]^-$ ions. $[HP_2O_5]^-$ ion at m/z 143 is the most characteristic product ion shown by all eight ESI-MS^2 spectra, formed spontaneously from the four-membered ring ion with P–O–P by loss of an aldehyde. $[HP_2O_5]^-$ ion at m/z 143 can hopefully be treated as a diagnostic ion of bisphosphonate group. Besides typical fragment ions of all the BPs, chloroacetyl Alendronate, chloroacetyl Pamidronate and Risedronate showed some additional fragmentation ions, containing triple bond ions owing to elimination of water from their enol anions. The hydrogen/deuterium (H/D) exchange experiment, theoretical calculations and the high-resolution mass spectrometry (Q-TOF) were appropriately employed to rationalize the proposed fragmentation pathways. These observations may have some potential applications in the structural elucidation and interpretation of mass spectra of nitrogen-containing bisphosphonate derivatives.

Acknowledgements

The authors would like to thank the National Natural Science Foundation of China (20472076 and 20972130) and Henan Aca-

demic Foundation of Science and Technology (No. 0512001400) for their financial support.

References

[1] H. Fleisch, in: W.A. Peck (Ed.), Bone and Mineral Research Annual 1, Excerpta Medica, Amsterdam, 1982, pp. 319–357.
[2] O.L.M. Bijvoet, H.A. Fleisch, R.E. Canfield, R.G.G. Russell (Eds.), Bispbosphonate on Bones, Amsterdam, Elsevier, 1995, pp. 111–124.
[3] G.A. Rodan, H.A. Fleisch, Bisphosphonates: mechanisms of action, J. Clin. Invest. 97 (1996) 2692–2696.
[4] D.E. Hughes, K.R. Wright, H.L. Uy, A. Sasaki, T. Yoneda, G.D. Roodman, Bisphosphonates promote apoptosis in murine osteoclasts in vitro and in vivo, J. Bone Miner. Res. 10 (1995) 1478–1487.
[5] E. Socrates, M.D. Papapoulos, Bisphosphonates: how do they work? Best Pract. Res. Clin. Endocrinol. Metab. 22 (2008) 831–847.
[6] E. Van Beek, M. Hoekstra, M. van de Ruit, C.W.G.M. Lowik, S.E. Papapoulos, Strucural requirements for bisphosphonate actions in vitro, J. Bone Miner. Res. 9 (1994) 1875–1882.
[7] E.R. van Beek, C. Lowik, F.H. Ebetino, Binding and antiresorptive properties of heterocycle-containing bisphosphonate analogs, Bone 23 (1998) 437–442.
[8] C.T. Leu, E. Luegmayr, L.P. Freedman, Relative binding affinities of bisphosphonates for human bone and relationship to antiresorptive efficacy, Bone 38 (2006) 628–636.
[9] E. Breuer, in: J. Fischer, C.R. Ganellin (Eds.), The Development of Bisphosphonates as Drugs, Wiley, Weinheim, 2006, pp. 371–384.
[10] A.A. Reszka, G.A. Rodan, Nitrogen-containing bisphosphonate mechanism of action, Mini. Rev. Med. Chem. 7 (2004) 711–719.
[11] E.V. Beek, L. Cohen, I. Leroy, F. Ebetino, C. Löwik, S. Papapoulos, Differentiating the mechanisms of antiresorptive action of nitrogen containing bisphosphonates, Bone 33 (5) (2003) 805–811.
[12] Z.Y. Ju, Y. Ye, D.H. Wei, R.Y. Zou, Y.F. Zhao, Electrospray ionization multistage tandem mass spectrometry of penta- and hexa-substituted aryloxycyclotriphosphazenes, Int. J. Mass Spectrom. 288 (2009) 51–57.
[13] P.R. Tiller, C. Raab, C.E.C.A. Hop, J. Mass Spectrom. 36 (2001) 344–345.
[14] Y. Jin, Y.W. Yin, H. Fu, Y.Y. Jiang, Y.F. Zhao, Analysis of Peptide mixtures through convenient isotopic labeling and electrospray ionization-mass spectrometry, Int. J. Mass Spectrom. 248 (2006) 108–114.
[15] K. Huikko, T. Kotiaho, J.Y. Kauhaluoma, R. Kostiainen, Electrospray ionization mass spectrometry and tandem mass spectrometry of clodronate and relatedbisphosphonate and phosphonate compounds, J. Mass Spectrom. 37 (2002) 197.
[16] M. Lecouvey, Y. Leroux, Synthesis of 1-hydroxy-1,1-bisphosphonates, Heteroatom. Chem. 11 (2000) 556–561.
[17] M.J. Frisch, G.W. Trucks, H.B. Schlegel, G.E. Scuseria, M.A. Robb, J.R. Cheeseman, J.A. Montgomery, T. Vreven Jr., K.N. Kudin, J.C. Burant, J.M. Millam, S.S. Iyengar, J. Tomasi, V. Barone, B. Mennucci, M. Cossi, G. Scalmani, N. Rega, G.A. Petersson, H. Nakatsuji, M. Hada, M. Ehara, K. Toyota, R. Fukuda, J. Hasegawa, M. Ishida, T. Nakajima, Y. Honda, O. Kitao, H. Nakai, M. Klene, X. Li, J.E. Knox, H.P. Hratchian, J.B. Cross, C. Adamo, J. Jaramillo, R. Gomperts, R.E. Stratmann, O. Yazyev, A.J. Austin, R. Cammi, C. Pomelli, J.W. Ochterski, P.Y. Ayala, K. Morokuma, G.A. Vot, P. Salvador, J.J. Dannenberg, V.G. Zakrzewski, S. Dapprich, A.D. Daniels, M.C. Strain, O. Farkas, D.K. Malick, A.D. Rabuck, K. Raghavachari, J.B. Foresman, J.V. Ortiz, Q. Cui, A.G. Baboul, S. Clifford, J. Cioslowski, B.B. Stefanov, G. Liu, A. Liashenko, P. Piskorz, I. Komaromi, R.L. Martin, D.J. Fox, T. Keith, M.A. AlLaham, C.Y. Peng, A. Nanayakkara, M. Challacombe, P.M.W. Gill, B. Johnson, W. Chen, M.W. Wong, C. Gonzalez, J.A. Pople, Gaussian 03, Revision C. 02, Gaussian, Inc., Wallingford, CT, 2004.
[18] J.R. Green, Antitumor effects of bisphosphonates, Cancer 97 (2003) 840–847.
[19] K.H.M. Cardozo, R. Vessecchi, V.M. Carvalho, E. Pinto, P.J. Gates, P. Colepicolo, S.E. Galembeck, N.P. Lopes, A theoretical and mass spectrometry study of the fragmentation of mycosporine-like amino acids, Int. J. Mass Spectrom. 273 (2008) 11–19.